

Unexpected Reconstruction of the α -Boron (111) Surface

Xiang-Feng Zhou,^{1,2,*} Artem R. Oganov,^{2,3,4} Xi Shao,¹ Qiang Zhu,² and Hui-Tian Wang^{1,5}

¹*School of Physics and Key Laboratory of Weak-Light Nonlinear Photonics, Nankai University, Tianjin 300071, China*

²*Department of Geosciences, Center for Materials by Design,
and Institute for Advanced Computational Science,*

Stony Brook University, Stony Brook, New York 11794, USA

³*Moscow Institute of Physics and Technology, 9 Institutskiy lane,
Dolgoprudny city, Moscow Region 141700, Russian Federation*

⁴*School of Materials Science, Northwestern Polytechnical University, Xi'an 710072, China*

⁵*National Laboratory of Solid State Microstructures, Nanjing University, Nanjing 210093, China*

We report on a novel reconstruction of the α -boron (111) surface, discovered using an *ab initio* evolution structure search, and reveal that it has an unexpected neat structure and much lower surface energy than the recently proposed (111)-I_{R,(a)} surface. For this reconstruction, every single interstitial boron atom forms bridges with the unique polar-covalent bonds between neighboring B_{12} icosahedra, which perfectly meet the electron counting rule and are responsible for the reconstruction-induced metal-semiconductor transition. The peculiar charge transfer between the interstitial atoms and the icosahedra plays an important role in stabilizing the surface.

PACS numbers: 68.35.bg, 71.15.Mb, 73.20.At

The element boron has been attracting an enormous amount of attention owing to its fascinating properties, such as fascinating structural complexity, superhardness, unusual partially ionic bonding, and superconductivity at high pressure [1–5]. As a neighbor for carbon, boron is in many ways an analog of carbon and its nanostructures (clusters, nanotubes, nanowires, nanobelts, fullerenes and so on) have aroused extensive interest, in the hopes also replicating or even surpassing the unique properties and diversity of carbon [6–12]. In analogy to graphene [13, 14], two dimensional (2D) boron sheets with the triangular and hexagonal motifs are predicted to be the most stable phases and likely precursors for boron nanostructures [15–22]. However, buckled bilayer structures appeared to be massively more stable; some of them turned out to have novel electronic properties, such as a distorted Dirac cone [23]. Surprisingly, there are a few studies on the boron surface with the dimension between bulk and 2D sheets. Hayami and Otani systematically studied the energies of low index bare surfaces in the α -boron, β -boron, and two tetragonal phases (t-I and t-II), which suggested that t-I and t-II can be more stable than α -boron and β -boron for sufficiently small nanoparticles [24, 25]. Amsler *et al.* took the first big step on the reconstruction of the α -boron (111) surface. Several low energy surface reconstructions were predicted by using the minima hopping method. In particular, a metallic reconstructed phase of (111)-I_{R,(a)} was predicted to be the most stable configuration, where a conducting boron sheet was adsorbed on a semiconducting substrate, leading to numerous possible applications in nanoelectronics [26]. However, this seems to be in conflict with the general principle that the reconstructions usually lower their energies by atomic rearrangement leading to semiconducting (as opposed to metallic) surface state [27].

Such an unexpected metallic reconstruction encourages us to explore other likely reconstructions and the stabilization mechanisms by first-principles calculations.

α -boron structure is composed of B_{12} icosahedra [28], has two inequivalent atomic sites, polar (B_p) and equatorial (B_e) sites, the B_p atoms form upper and lower triangles of an icosahedron and the B_e atoms form a waving hexagon along the equator of an icosahedron [2]. The arrangement of icosahedra in α -boron can be described as a cubic close packing with the layer sequence ABC [1]. Compared with the (111)-I_{R,(a)} surface that built along [111] direction of the primitive rhombohedral cell with the surface vectors $\mathbf{U}(2\bar{1}\bar{1})$ and $\mathbf{V}(11\bar{2})$, we cleaved the surface along [111] direction with the surface vectors $\mathbf{U}(\bar{1}\bar{1}\bar{2})$ and $\mathbf{V}(1\bar{1}0)$, which allowed us to reduce the required computational resource drastically. The calculations were conducted on the 4 layered B_{12} icosahedra of the (111)-I substrate, and then (111)-II substrate was also tested [25, 26]. In both cases we obtained exactly the same reconstruction, regardless the type of substrate if enough atoms and thickness are used. Structure searches for the reconstructions were performed using the *ab initio* evolutionary algorithm USPEX [29–31], which has been successfully applied to various materials [32–34]. The number of surface atoms was allowed to vary from 1 to 20 with the vacuum layer of 10 Å, which are restricted to the surface layer of thickness 4 Å. Given that the thickness of B_{12} icosahedron is ~ 3.7 Å, there is an enough space to fully explore the chemical landscape in our calculations. The all-electron projector-augmented wave method [35] was employed, as implemented in the Vienna *ab initio* simulation package (VASP) [36] with the generalized gradient approximation (GGA) and the functional of Perdew, Burke, and Ernzerhof (PBE) [37]. A plane-wave cutoff energy of 500 eV and a Monkhorst-Pack Brill-

loun zone sampling grid with resolution $2\pi \times 0.04 \text{ \AA}^{-1}$ were used. In addition, the hybrid HSE06 functional with the screening parameter (ω) 0.2 \AA^{-1} was also employed to check the robustness of surface energies [38].

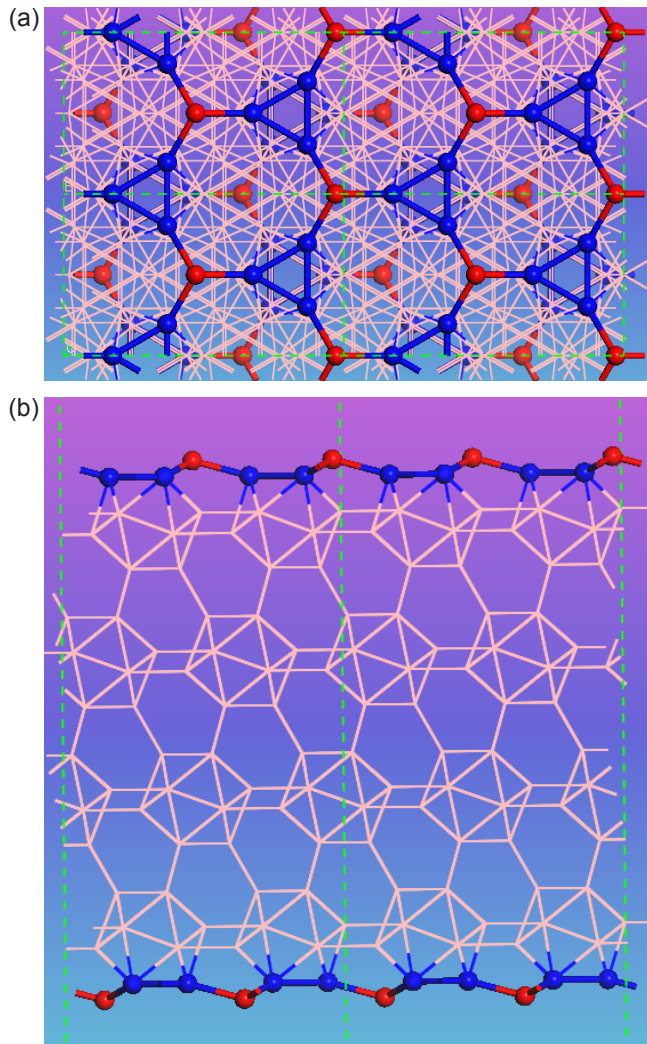


FIG. 1. (Color online) (a) Projection of $2 \times 2 \times 1$ supercell of the $(111)\text{-I}_{R,(z)}$ structure along $[111]$ direction. (b) projection of $2 \times 2 \times 1$ supercell of the $(111)\text{-I}_{R,(z)}$ structure along $[\bar{1}\bar{1}\bar{2}]$ direction. The nonequivalent surface atoms are shown by different colors.

For the most stable $(111)\text{-I}_{R,(a)}$ surface, there is buckling and coupling among three outer atomic layers above the icosahedral B_{12} units, which result in structural complexity [26]. In contrast to $(111)\text{-I}_{R,(a)}$, our reconstruction [designated as $(111)\text{-I}_{R,(z)}$] has an unexpected neat structure, as shown in Fig. 1(a), where a single boron atom occupies the interstitial position (named as B_i , colored in red), connects the B_p atoms (colored in blue) and forms bridges with bond lengths of 1.793 \AA and bond angles of 113.06° . The B_i atoms are slightly above the topmost icosahedral atoms (B_p), see Fig. 1(b), which form

TABLE I. The surface energies of the unreconstructed $(111)\text{-I}$, reconstructed $(111)\text{-I}_{R,(a)}$, and $(111)\text{-I}_{R,(z)}$ structures by using different functionals, in units of $\text{meV}/\text{\AA}^2$.

Surface	$(111)\text{-I}$	$(111)\text{-I}_{R,(a)}$	$(111)\text{-I}_{R,(z)}$	Reference
PBE	219.29	170.64	128.23	This work
	218.80	170.61		26
HSE	248.43	197.39	136.79	This work
	247.50	196.31		26

the modulated “3 + 9” membered rings on the topmost surface. Interestingly, the $(111)\text{-I}_{R,(z)}$ and $(111)\text{-I}_{R,(a)}$ share almost the same surface motif (3 + 9 structure), which hints that the $(111)\text{-I}_{R,(a)}$ surface may be a local metastable phase. According to the surface energy $\sigma = (1/2A)(N\epsilon_{bulk} - E_{slab})$, where A denotes the surface area, ϵ_{bulk} is the energy per atom in the bulk α -boron and E_{slab} is the energy of the substrate containing N atoms [26]. We calculate the surface energies of $(111)\text{-I}$ and $(111)\text{-I}_{R,(a)}$ by using the GGA-PBE and HSE06 methods, as listed in the Table I, which are in excellent agreement with previous results [26]. This establishes the reliability and accuracy of our calculations. Strikingly, the surface energy of $(111)\text{-I}_{R,(z)}$ is $128.23 \text{ meV}/\text{\AA}^2$ for GGA-PBE and $136.79 \text{ meV}/\text{\AA}^2$ for HSE06, which is considerably, by 42 and $60 \text{ meV}/\text{\AA}^2$ respectively, lower in energy than the $(111)\text{-I}_{R,(a)}$ structure. To confirm the most stable surface, we also perform the structure search with the same substrate proposed by Ref. [26], get the same reconstruction and energy, and find there is no dependence on the choice of the surface vectors/cleavage plane: it is the general rule that the ratio of B_i to the exposed B_{12} icosahedron should be 1 : 1 in α -boron (111) surface.

Figure 2 shows the band structures of the unreconstructed $(111)\text{-I}$ and the reconstructed $(111)\text{-I}_{R,(z)}$ surfaces from the GGA-PBE calculations. Due to the unsaturated dangling bonds, the $(111)\text{-I}$ surface is metallic, as shown in Fig. 2(a). In contrast, Figure 2(b) shows the $(111)\text{-I}_{R,(z)}$ surface is a semiconductor with a direct DFT band gap of 1.13 eV compared with the band gap of 1.50 eV for bulk α -boron. The reconstruction-induced metal-semiconductor transition meets the general principle that reconstructions usually lower their energies by atomic rearrangements leading to semiconducting surface state [27]. According to Wade’s rule [39, 40], a B_{12} icosahedron has 36 valence electrons, 26 of which may be used for intricosahedral bonds and 10 for intericosahedral bonds. Each icosahedron forms six two-electron-two-center (2e2c) bonds with the icosahedra of neighboring layers, which requires $6 \times 2/2 = 6$ electrons, as well as six closed two-electron-three-center (2e3c) bonds with the neighboring icosahedra in its own layer, these multi-center bonds require $6 \times 2/3 = 4$ electrons [1]. The $(111)\text{-I}$ surface cuts three intericosahedral bonds (2e2c) per icosahedron.

hedron, and there are two B_{12} icosahedra per stacking layer in the (111)- $I_{R,(z)}$ surface. Therefore, the unsaturated dangling bonds of the (111)- $I_{R,(z)}$ surface need additional $3 \times 2 \times 2/2 = 6$ valence electrons. Two B_i atoms are just added to the surface, connect six B_p atoms, as shown in Fig. 1(a), form six bridging B-B bonds (these are the closed $2e2c$ bonds, may not the same), which perfectly satisfy the electron counting rule (ECR) [27, 41], and are responsible for the reconstruction-induced metal-semiconductor transition.

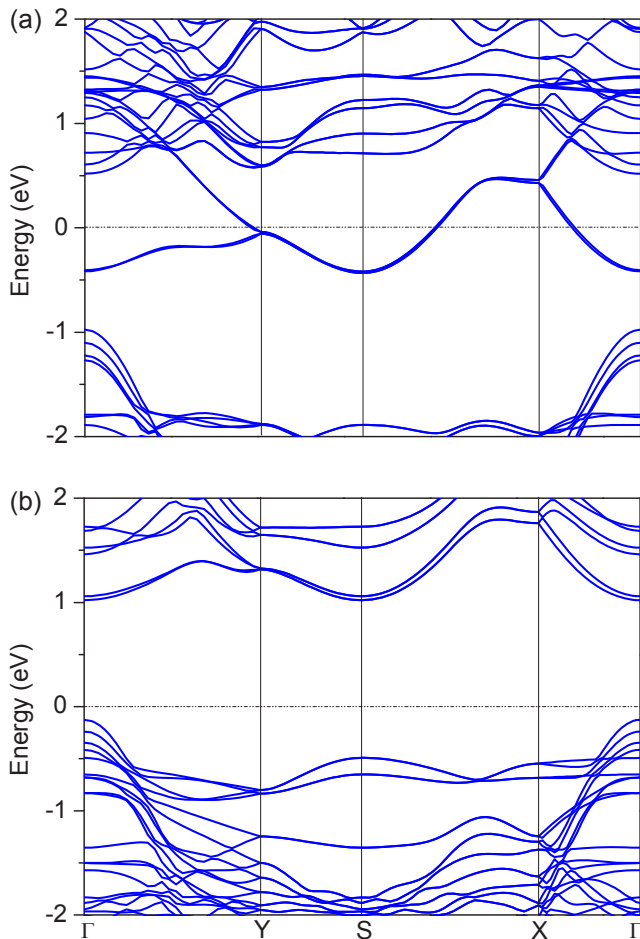


FIG. 2. (Color online) Band structures of (a) (111)-I and (b) (111)- $I_{R,(z)}$, the special k points are labeled as $\Gamma(0\ 0\ 0)$, $Y(0\ 0.5\ 0)$, $S(-0.5\ 0.5\ 0)$, and $X(-0.5\ 0\ 0)$, respectively.

Projected density of states (PDOS) of the topmost atoms is plotted in Fig. 3. The (111)-I surface exhibits metallic character, see Fig. 3(a), dominantly due to the out-of-plane states (p_z orbitals), arising from the unsaturated B_p atoms, and located near the bottom of the conduction band. In comparison, strongly hybridized bonding states present in the vicinity of the Fermi level in Fig. 3(b), mainly derive from the B_p : p_z and B_i : p_{xy} orbitals, and are fully filled. The (111)- $I_{R,(z)}$ surface is thereby a semiconductor. PDOS (Figs. 3c and 3d)

clearly shows the out-of-plane p_z states and the in-plane p_{xy} states near the valence band edge are dominantly from the B_p and B_i atoms, respectively. Because the B_i atoms are located above empty space, there is no p_z state for the B_i under the Fermi level in Fig. 3(d). Moreover, the distance between the B_i and B_e atoms is 2.926 Å. All of these facts indicate that there is no interaction/bonding between the B_i and B_e atoms, which further confirms the reliability of the surface bonding configuration and the ECR applied for the (111)- $I_{R,(z)}$ surface.

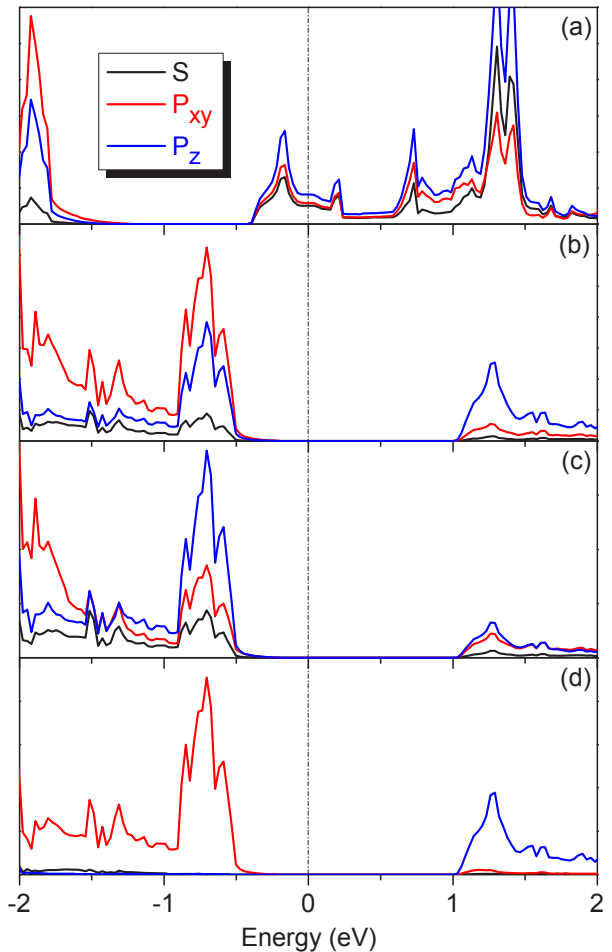


FIG. 3. (Color online) [(a) and (b)] PDOS of the (111)-I and (111)- $I_{R,(z)}$ structures. [(c) and (d)]PDOS of the B_p and B_i atoms in (111)- $I_{R,(z)}$ structure.

Symmetry breaking of B_{12} icosahedra results in charge asymmetry on some B-B bonds, and in fact a small degree of ionicity of B-B bonds in the B_{12} icosahedron was predicted in α -boron [3], while a much greater degree of ionicity was found in the high pressure partially ionic γ phase [4]. It is extremely important and interesting to study the charge transfer/ionicity for the (111)- $I_{R,(z)}$ surface. Figure 4 shows the charge density difference between B_i and B_p atoms [42]. There is a notable

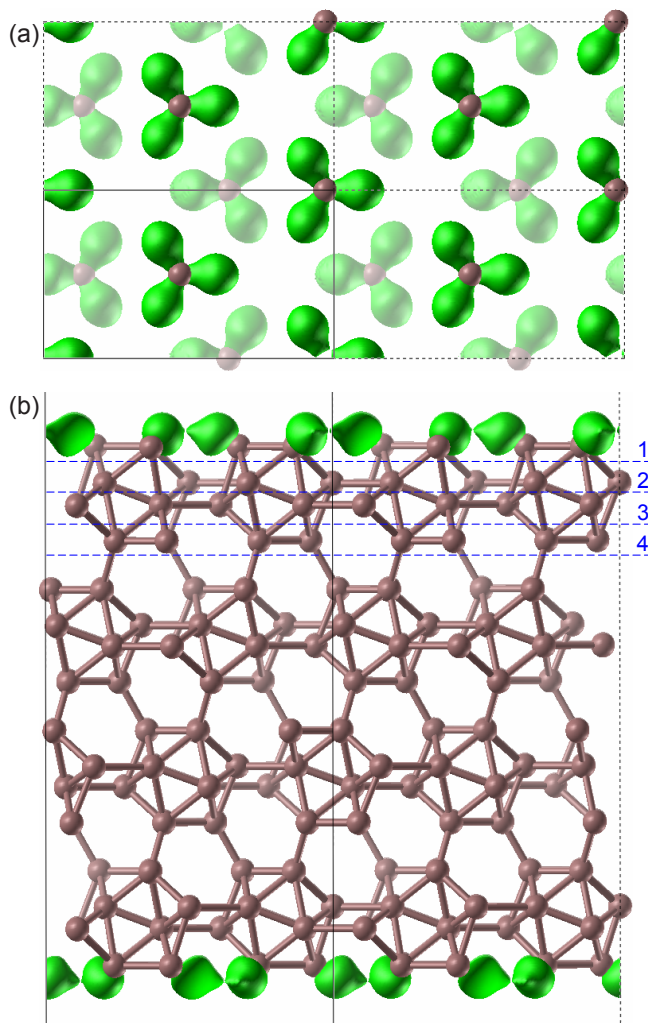


FIG. 4. (Color online) (a) Projection of the charge density difference of the (111)- $I_{R,(z)}$ structure along [111] direction. (b) projection of the charge density difference of the (111)- $I_{R,(z)}$ structure along $[\bar{1}\bar{1}2]$ direction. The top four atomic layers are labeled from 1 to 4.

charge transfer from B_i to the neighboring B_{12} icosahedra through B_p atoms. Bader charges for B_i is $+0.17e$, and $+0.04e$ for B_p [43]. Strikingly, the charge transfer keeps the charge state of B_p close to its bulk state ($\sim +0.05e$) [4, 23], and the significant charge transfer between the B_i and B_{12} icosahedra indicates the bridging B_i - B_p bonds are unique polar covalent bonds, which contrasted sharply with the intericosahedral purely covalent B_p - B_p bonds [3]. Due to the charge transfer, the B_i - B_p bonds (1.793 Å) are much weaker and longer than the B_p - B_p bonds (1.673 Å). In Fig. 4(b), each B_{12} icosahedron comprises 4 atomic layers (labeled from 1 to 4), the charge transfer for these 4 layers should be in the “+ - - +” order with the values of $+0.56$, -0.46 , -0.46 , and $+0.36e$, compared with the corresponding values of $+0.20$, -0.22 , -0.22 , and $+0.24e$ in α -boron. It is clear

from these numbers that the surface region as a whole is charge-neutral. The charge transfer of the (111)- $I_{R,(z)}$ surface is rebalanced within the top 4 atomic layers (include the B_i atoms and the B_{12} icosahedra), which plays an important role in stabilizing the surface.

In conclusion, the most simple and stable reconstructions of the α -boron (111) surface has been investigated in detail using *ab initio* evolutionary structure search. Our results show the (111)- $I_{R,(z)}$ surface is lower in energy than the earlier reported structures [26], and confirm that the classical ECR governs the reconstructions, results in the formation of novel bridging bonds between the B_i and B_p atoms, leading to the metal-semiconductor transition. In particular, significant charge transfer is responsible for the unique polar-covalent bonds between the B_i and B_p atoms. Charge redistribution between the B_i atoms and the B_{12} icosahedra is one of the key factors stabilizing the reconstruction.

X.F.Z. thanks Philip B. Allen and Maria V. Fernandez-Serra for valuable discussions. This work was supported by the National Science Foundation of China (Grants No. 11174152 and No. 91222111), the National 973 Program of China (Grant No. 2012CB921900), the Program for New Century Excellent Talents in University (Grant No. NCET-12-0278), and the Fundamental Research Funds for the Central Universities (Grant No. 65121009). A.R.O. thanks the National Science Foundation (EAR-1114313, DMR-1231586), DARPA (Grants No. W31P4Q1310005 and No. W31P4Q1210008), DOE (Computational Materials and Chemical Sciences Network (CMCSN) project DE-AC02-98CH10886), CRDF Global (UKE2-7034-KV-11), AFOSR (FA9550-13-C-0037), the Government (No. 14.A12.31.0003) and the Ministry of Education and Science of Russian Federation (Project No. 8512) for financial support, and Foreign Talents Introduction and Academic Exchange Program (No. B08040). Calculations were performed on XSEDE facilities and on the cluster of the Center for Functional Nanomaterials, Brookhaven National Laboratory, which is supported by the DOE-BES under contract no. DE-AC02-98CH10086.

* xfzhou@nankai.edu.cn; zxf888@163.com

- [1] B. Albert and H. Hillebrecht, *Angew. Chem. Int. Ed.* **48**, 8640 (2009).
- [2] M. Fujimori, T. Nakata, T. Nakayama, E. Nishibori, K. Kimura, M. Takata, and M. Sakata, *Phys. Rev. Lett.* **82**, 4452 (1999).
- [3] J. He, E. Wu, H. Wang, R. Liu, and Y. J. Tian, *Phys. Rev. Lett.* **94**, 015504 (2005).
- [4] A. R. Oganov, J. H. Chen, C. Gatti, Y. Z. Ma, Y. M. Ma, C. W. Glass, Z. X. Liu, T. Yu, O. O. Kurakevych, and V. L. Solozhenko, *Nature (London)* **457**, 863 (2009).
- [5] M. I. Erements, V. V. Struzhkin, Ho-kwang Mao, and R. J. Hemley, *Science* **293**, 272 (2001).

- [6] H. J. Zhai, B. Kiran, J. Li, and L. S. Wang, *Nat. Mater.* **2**, 827 (2003).
- [7] F. Liu, C. Shen, Z. Su, X. Ding, S. Deng, J. Chen, N. Xu, and H. Gao, *J. Mater. Chem.* **20**, 2197 (2010).
- [8] C. J. Otten, O. R. Lourie, M. F. Yu, J. M. Cowley, M. J. Dyer, R. S. Ruoff, and W. E. Buhro, *J. Am. Chem. Soc.* **124**, 4564 (2002).
- [9] Y. Sato, M. Terauchi, K. Kirihara, T. Sasaki, K. Kawaguchi, N. Koshizaki, and K. Kimura, *J Phys Conf Ser.* **176**, 012029 (2009).
- [10] N. Gonzalez Szwacki, A. Sadrzadeh, and B. I. Yakobson, *Phys. Rev. Lett.* **98**, 166804 (2007).
- [11] Dasari L. V. K. Prasad and Eluvathingal D. Jemmis, *Phys. Rev. Lett.* **100**, 165504 (2008).
- [12] S. De, A. Willand, M. Amsler, P. Pochet, L. Genovese, and S. Goedecker, *Phys. Rev. Lett.* **106**, 225502 (2011).
- [13] K. S. Novoselov, A. K. Geim, S.V. Morozov, D. Jiang, M. I. Katsnelson, I.V. Grigorieva, S.V. Dubonos, and A. A. Firsov, *Nature (London)* **438**, 197 (2005).
- [14] A. K. Geim, *Science* **324**, 1530 (2009).
- [15] I. Boustani, *Surf. Sci.* **370**, 355 (1997).
- [16] I. Boustani, *Phys. Rev. B* **55**, 16426 (1997).
- [17] H. Tang and S. Ismail-Beigi, *Phys. Rev. Lett.* **99**, 115501 (2007).
- [18] A. Sebetci, E. Mete, and I. Boustani, *J. Phys. Chem. Solids* **69**, 2004 (2008).
- [19] H. Tang and S. Ismail-Beigi, *Phys. Rev. B* **80**, 134113 (2009); *Phys. Rev. B* **82**, 115412 (2010).
- [20] S. Saxena, and T. A. Tyson, *Phys. Rev. Lett.* **104**, 245502 (2010).
- [21] E. S. Penev, S. Bhowmick, A. Sadrzadeh, and B. I. Yakobson, *Nano Lett.* **12**, 2441 (2012).
- [22] X. Wu, J. Dai, Y. Zhao, Z. Zhuo, J. Yang, and X. C. Zeng, *ACS Nano* **6**, 7443 (2012).
- [23] X. F. Zhou, X. Dong, A. R. Oganov, Q. Zhu, Y. Tian, and H. T. Wang, *Phys. Rev. Lett.* **112**, 085502 (2014).
- [24] W. Hayami and S. Otani, *J. Phys. Chem. C* **111**, 10 394 (2007).
- [25] W. Hayami and S. Otani, *J. Phys. Chem. C* **111**, 688 (2007).
- [26] M. Amsler, S. Botti, Miguel A. L. Marques, and S. Goedecker, *Phys. Rev. Lett.* **111**, 136101 (2013).
- [27] C. B. Duke, *Chem. Rev.* **96**, 1237 (1996).
- [28] B. F. Decker and J. S. Kasper, *Acta Cryst.* **12**, 503 (1959).
- [29] A. R. Oganov and C. W. Glass, *J. Chem. Phys.* **124**, 244704 (2006).
- [30] C. W. Glass, A. R. Oganov, and N. Hansen, *Comput. Phys. Commun.* **175**, 713 (2006).
- [31] Q. Zhu, L. Li, A. R. Oganov, and P. B. Allen, *Phys. Rev. B* **87**, 195317 (2013).
- [32] X. F. Zhou, A. R. Oganov, X. Dong, L. Zhang, Y. Tian, and H. T. Wang, *Phys. Rev. B* **84**, 054543 (2011).
- [33] X. F. Zhou, A. R. Oganov, G. R. Qian, and Q. Zhu, *Phys. Rev. Lett.* **109**, 245503 (2012).
- [34] C. H. Hu, A. R. Oganov, Q. Zhu, G. R. Qian, G. Frapper, A. O. Lyakhov, and H. Y. Zhou, *Phys. Rev. Lett.* **110**, 165504 (2013).
- [35] P. E. Blöchl, *Phys. Rev. B* **50**, 17953 (1994).
- [36] G. Kresse and J. Furthmüller, *Phys. Rev. B* **54**, 11169 (1996); *Comput. Mater. Sci.* **6**, 15 (1996).
- [37] J. P. Perdew, K. Burke, and M. Ernzerhof, *Phys. Rev. Lett.* **77**, 3865 (1996).
- [38] J. Heyd, G. E. Scuseria, and M. Ernzerhof, *J. Chem. Phys.* **118**, 8207 (2003).
- [39] K. Wade, *Adv. Inorg. Chem. Radiochem.* **18**, 1 (1976).
- [40] E. D. Jemmis, M. M. Balakrishnarajan, and P. D. Pancharatna, *J. Am. Chem. Soc.* **123**, 4313 (2001).
- [41] M. D. Pashley, *Phys. Rev. B* **40**, 10481 (1989).
- [42] The charge density difference $\delta\rho = \rho_{AB} - (\rho_A + \rho_B)$, where ρ_{AB} is the charge density of the (111)- $I_{R,(z)}$ surface, ρ_A is the charge density of the B_i atoms, and ρ_B is the charge density of the unrelaxed structure which the B_i atoms are removed from the (111)- $I_{R,(z)}$ surface.
- [43] W. Tang, E. Sanville, and G. Henkelman, *J. Phys. Condens. Matter* **21**, 084204 (2009).